



# Sol-Gel Synthesis, Magnetic and Optical Properties of $\text{Co}^{2+}:\text{Nd}^{3+}::2:1$ molar ratio doped in $\text{SiO}_2$

Bidhu Bhusan Das, Ruppa Govinda Rao

Functional Materials Chemistry Laboratory, Department of Chemistry,

Pondicherry University, Pondicherry-605014 (India)

E-mail: [das\\_b\\_b@yahoo.com](mailto:das_b_b@yahoo.com)

## ABSTRACT

Synthesis of  $\text{Co}^{2+}:\text{Nd}^{3+}::2:1$  molar ratio doped  $\text{SiO}_2$  with  $\text{Co}^{2+}$  ions concentrations viz. 0.0004, 0.001, 0.002, 0.003, 0.004 moles in S1-S5, respectively are performed by sol-gel method. Observed values of the densities and the concentrations of the  $\text{Co}^{2+}$  ions in S1-S5 are found to be 2.26, 2.29, 2.37, 3.44, 2.49  $\text{g/cm}^3$ , and  $\sim 10^{20}$  ions/g, respectively. Powder XRD results show the formation of amorphous  $\text{SiO}_2$  phase in the samples. DTA-TGA/DTG traces in the range 27-700  $^\circ\text{C}$  show no characteristic event in the samples. The IR peak in the range 412-418  $\text{cm}^{-1}$  is ascribed to the asymmetric mode of the octahedral  $[\text{NdO}_6]^{3-}$  units. The peak around 440  $\text{cm}^{-1}$  in S1-S5 is due to the  $\nu_2$ -symmetric bending mode of the tetrahedral  $[\text{SiO}_4]^{4-}$  units. The weak IR peak  $\sim 670 \text{ cm}^{-1}$  is due to the  $\nu_1$ -mode of the tetrahedral  $[\text{CoO}_4]^{4-}$  units. The calculated values of the magnetic susceptibility from the observed magnetic moments data at 300 K are found to be  $\sim 10^{-6}$  emu/gG in S1-S5 which show the weak paramagnetic nature of the materials. The EMR lineshapes recorded at 6, 50, 77, and 300 K are very broad, isotropic and smeared out with only two detectable characteristic peaks. The  $g_{\text{iso}}$ -value  $\sim 2.3$  is due to the doped  $\text{Co}^{2+}(3d^7)$  ions in tetrahedral coordinations, while the  $g_{\text{iso}}$ -value  $\sim 2.01$  is due to the doped  $\text{Nd}^{3+}(4f^3)$  ions in distorted octahedral coordinations. The lineshapes only at 6 K are distinct, while at higher temperatures these peaks are severely smeared out. The optical absorption broad band at  $\sim 750 \text{ nm}$  ( $13262 \text{ cm}^{-1}$ ) is assigned to  $^4\text{I}_{9/2} \rightarrow ^4\text{F}_{7/2} + ^4\text{S}_{3/2}$  transitions in optically active  $\text{Nd}^{3+}(4f^3)$  ions, and the peak  $\sim 520 \text{ nm}$  ( $19230 \text{ cm}^{-1}$ ) is attributed to  $^4\text{A}_{2g} \rightarrow ^4\text{T}_{1g}(\text{P})$  transitions in  $\text{Co}^{2+}(\text{S}=3/2, 3d^7)$  ions in tetrahedral coordinations.

## Indexing terms/Keywords

sol-gel method;  $\text{SiO}_2$ ; electron magnetic resonance (EMR); magnetic measurements

## Academic Discipline And Sub-Disciplines

Chemistry: Physical chemistry

## SUBJECT CLASSIFICATION

Materials chemistry

## TYPE (METHOD/APPROACH)

Experimental

# Council for Innovative Research

Peer Review Research Publishing System

**Journal:** Journal of Advances in Chemistry

Vol. 11, No. 3

[editorjaconline@gmail.com](mailto:editorjaconline@gmail.com)

[www.cirjac.com](http://www.cirjac.com)



## 1. INTRODUCTION

Nanosize materials and the application of nanotechnology is the thrust area of research in materials chemistry and physics, because of their wide application potentials. One of the important class of nanomaterials is the metal ion-doped (transition metal or rare earth elements) zinc silicate nanophosphor ( $\text{Zn}_2\text{SiO}_4\text{:X}$ ) ( $\text{X}=\text{Mn}^{2+}$ ,  $\text{Eu}^{3+}$  etc.) [1] and [2] because of their interesting optical and magnetic properties. Literature has also reports on the EMR [3], [4], [5], [6], [7], [8] and [9] and optical properties [10], [11] and [12] of  $\text{Co}^{2+}(3d^7)$  ions doped in various diamagnetic oxide matrices or in oxide matrices with other magnetic transition metal or rare-earth ions [13] in varied coordination geometries. We also reported earlier on EMR and optical properties of  $\text{Nd}^{3+}(4f^3)$  ions in diamagnetic oxide matrices [14] and [15].

There are varieties of preparative methods available for the nanosize materials depending of their usage. One of the most important and widely used method is the sol-gel process [16] and [17] for preparing the nanomaterials. In this paper, we report our method of sol-gel synthesis and the results of our studies on the Co- and Nd-doped silicon dioxide amorphous powder using varieties of structure-sensitive techniques such as, powder x-ray diffraction (XRD), differential thermal analysis (DTA)-thermogravimetric analysis (TGA)/derivative thermogravimetry (DTG), IR- and FT-Raman spectroscopy, magnetic measurements, optical absorptions, variable temperature electron magnetic resonance (EMR), chemical analysis and density measurements.

## 2. EXPERIMENTALS

### 2.1 Sample Preparation

In 10 g of tetraethoxysilane calculated amount of distill water and hydrochloric acid are added and stirred at  $\sim 60^\circ\text{C}$  for 1 h to convert it to silicon tetrachloride,  $\text{SiCl}_4$ . To the above solution, 20 ml of 1- propanal and 2-butanol each are added, and stirred for 1 h. To the resulting solution, viz. 0.0004 (0.06 g), 0.001 (0.2 g), 0.002 (0.35 g), 0.003 ( 0.5 g), 0.004 (0.65 g) mol (or weight in g) of finely powdered of cobalt acetate,  $\text{Co}(\text{CH}_3\text{COO})_2$ , and the corresponding moles of neodymium acetate,  $\text{Nd}(\text{CH}_3\text{COO})_3$ , in accordance with 2:1 molar ratio are added to prepare the Co- and Nd-doped five samples S1-S5, respectively. The resulting bulk solutions are stirred for 24 h. To the above solutions, then 20 ml of cyclohexane and liquor ammonia are added while stirring till the emulsion is formed around pH  $\sim 7.0$ . The resulting gel is decomposed by heating  $\sim 120^\circ\text{C}$  to fine powder, which is then sintered at  $850^\circ\text{C}$  for 4 h, and quenched in air to obtain the Co- and Nd-doped  $\text{SiO}_2$  nanosized powder.

### 2.2 Experimental Techniques

Powder x-ray diffraction patterns of the samples are recorded at 300 K on a X'pert (PAN Analytical) diffractometer using monochromatic Cu K $\alpha$  radiation ( $\lambda \sim 1.54056 \text{ \AA}$ ) in the range  $20^\circ$ - $70^\circ$  in  $2\theta$ . The x-ray tube is operated at 25 mA/ 40 kV with 1000 Watts x-ray power. The count rate is maintained at 1000 counts per second using a proportional counter. The differential thermal analysis (DTA)- thermogravimetric analysis (TGA)/ derivative thermogravimetric (DTG) data are collected in Mettler Toledo STARE System of module TGA/SDTA851e under static nitrogen atmosphere in the range range 27-700  $^\circ\text{C}$ . The IR spectra of the glasses are recorded at 300 K in the range  $400$ - $4000 \text{ cm}^{-1}$  by a SHIMADZU FT-IR-8700 spectrometer using "KBr pellet" technique [18]. FT-Raman spectra of the samples are recorded using an FT-IR/ FT-Raman Bruker IFS66V/FRA106 in the range  $50$ - $3500 \text{ cm}^{-1}$ . X-band EMR data are recorded at 6, 50 and at 300 K are recorded on a Varian E-122 spectrometer using an Air Products Helitran cryostat for low temperatures. The magnetic field is calibrated using with a Varian NMR Gauss meter and the microwave frequency is determined using an EIP frequency meter. Since a Gauss meter and frequency meter are used to record the EMR lineshapes in these cases, a g-standard is not necessary. The g-values can be computed directly from the spectra using the recorded value of the frequency and the resonance line position. X-band ESR spectral measurements at 77 K are done with a JEOL JES-TE 100 ESR spectrometer system with 100 kHz magnetic field modulation and a phase sensitive detector to obtain the first derivative signal. In order to measure the derivative EMR peak-to-peak linewidths variation as a function of composition in the samples, the lineshapes are recorded with sufficiently low microwave power to avoid saturation. The magnetic field calibration has been made with respect to the resonance line of DPPH ( $g_{\text{DPPH}} = 2.00354$ ) [19] at 77 K, which is used as a field 'marker'. The magnetic moments of the samples in emu at 300 K are measured using a vibrating sample magnetometer (VSM) (Model LAKESHORE - 7404 Series) in the cyclic magnetic field range  $\pm 10 \text{ kG}$ . The optical absorption spectra are recorded on a Varian Spectrophotometer (Model Carry 5000) in the range  $200$ - $780 \text{ nm}$  in the solid phase. Chemical analyses of the samples are done by wet chemistry method [20], and the densities are determined by liquid displacement method using n-dibutylphthalate as the immersion liquid (density  $1.043 \text{ g/cc}$  at 300 K).

## 3. RESULTS AND DISCUSSION

### 3.1 Powder XRD and Thermal studies

In Fig. 1 we show the powder XRD patterns of the samples S1-S5. The patterns show a broad peak at lower diffraction angles which vanishes at higher diffraction angles. This shows the amorphous nature of the samples due to the  $\text{SiO}_2$  network. In Table 1, we present the observed values of the densities and the chemical analyses results. A general trend of increase in the values of densities from  $2.26 \text{ g/cm}^3$  in S1 through  $2.49 \text{ g/cm}^3$  in S5 is observed with the increase in the concentrations of the  $\text{Co}^{2+}$  ions from S1 to S5. The DTA-TGA/DTG traces of S1-S5 in the range  $27$ - $700^\circ\text{C}$  show no significant phase transition as well as weight loss in the samples in the temperature range studied.

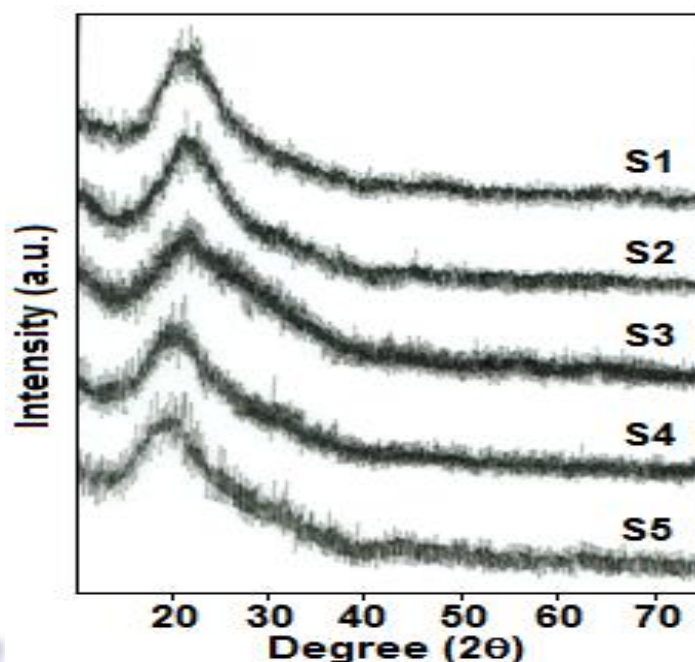


Fig. 1: Powder X-ray diffraction patterns of the samples S1-S5 of Co- and Nd-doped amorphous SiO<sub>2</sub> at 300 K

Table 1. Observed values of the densities and the concentrations of the Co<sup>+2</sup> and Nd<sup>3+</sup> ions and the calculated values of the magnetic susceptibility in the samples S1-S5 of Co- and Nd-doped amorphous SiO<sub>2</sub>

Sample No.	Density (g/cm <sup>3</sup> )	No. of Co <sup>2+</sup> ions (per g)	Magnetic susceptibility $\chi$ (emu/gG)	Conc. of (Nd <sup>3+</sup> + Co <sup>2+</sup> ) ions (per g)	Conc. of Nd <sup>3+</sup> ions (per g)
S1	2.26	$0.63 \times 10^{20}$	$2.52 \times 10^{-6}$	$0.90 \times 10^{20}$	$0.27 \times 10^{20}$
S2	2.29	$0.75 \times 10^{20}$	$6.22 \times 10^{-6}$	$1.10 \times 10^{20}$	$0.35 \times 10^{20}$
S3	2.37	$0.88 \times 10^{20}$	$5.62 \times 10^{-6}$	$1.30 \times 10^{20}$	$0.42 \times 10^{20}$
S4	2.44	$0.91 \times 10^{20}$	$5.48 \times 10^{-6}$	$1.33 \times 10^{20}$	$0.42 \times 10^{20}$
S5	2.49	$0.92 \times 10^{20}$	$11.4 \times 10^{-6}$	$1.13 \times 10^{20}$	$0.51 \times 10^{20}$

### 3.2 Infrared and FT-Raman spectra studies

In Figs. 2 and 3, we show the IR and FT-Raman spectra recorded at 300 K of S1-S5, respectively. The peaks up to 300 cm<sup>-1</sup> in the Raman spectra of the samples are ascribed to the lattice mode [21]. The very weak IR peak or shoulder in the range 412-418 cm<sup>-1</sup> in S1-S5 is attributed to the asymmetric stretching of octahedral [Nd<sub>06/2</sub>]<sup>3-</sup> units [22]. The IR peaks around 440 cm<sup>-1</sup> in S1-S5 is due to  $\nu_2$ -symmetric bending mode [21] of the tetrahedral [SiO<sub>4/2</sub>]<sup>4-</sup> units, and the strong IR peak ~ 470 cm<sup>-1</sup> in S1-S5 is due to the  $\nu_4$ -asymmetric bending [21] of the tetrahedral [SiO<sub>4/2</sub>]<sup>4-</sup> units. The Raman spectra of the samples also show peaks in the above ranges. The weak IR peak ~ 670 cm<sup>-1</sup> is due to the  $\nu_1$ -mode [23] of the tetrahedral [CoO<sub>4/2</sub>]<sup>4-</sup> units. The IR and Raman peaks ~ 800 cm<sup>-1</sup> in S1-S5 are due to the  $\nu_1$ -symmetric stretch [21] and [24] as well as symmetric bending [18] of O-Si-O bonds of the tetrahedral [SiO<sub>4/2</sub>]<sup>4-</sup> units. The very strong IR peak ~ 1100 cm<sup>-1</sup> is due to the  $\nu_3$ -asymmetric stretch [21] of the tetrahedral [SiO<sub>4/2</sub>]<sup>4-</sup> units. The Raman spectra also show lines in the range 900-1200 cm<sup>-1</sup> due to the above mode. The weak shoulder ~1210 cm<sup>-1</sup> is attributed to the asymmetric stretch [25] of O-Si-O bonds of the tetrahedral [SiO<sub>4/2</sub>]<sup>4-</sup> units.



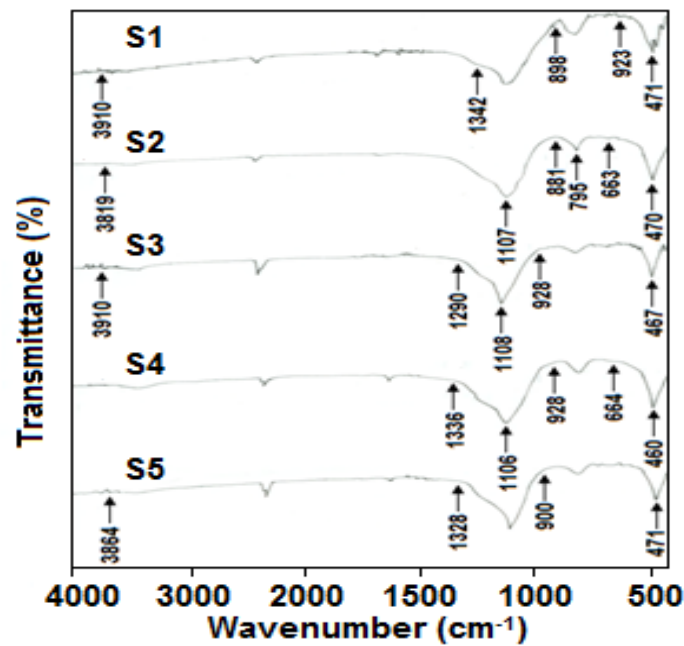


Fig. 2 : IR spectra of S1-S5 of Co- and Nd-doped SiO<sub>2</sub> at 300 K

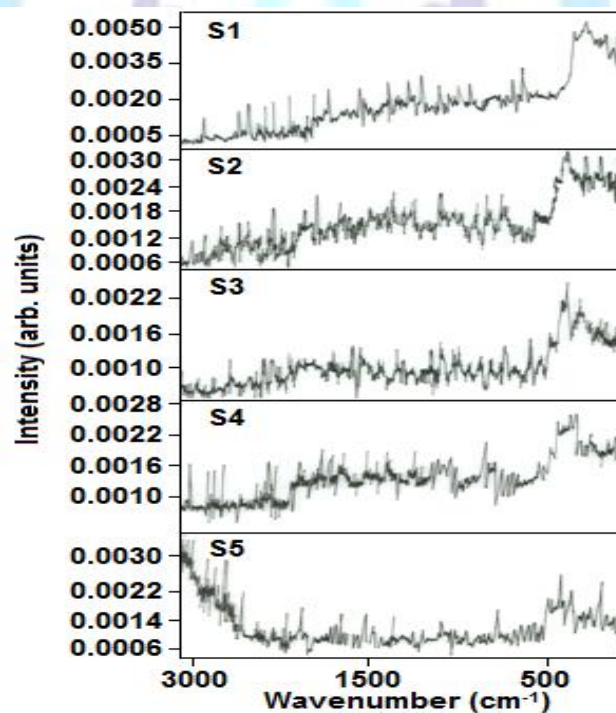


Fig. 3: FT-Raman spectra of S1-S5 of Co- and Nd-doped SiO<sub>2</sub> at 300 K

### 3.3 Magnetic Properties

In Fig. 4 we show the plot of magnetic moment versus magnetic field of the sample S1-S5 recorded at 300 K. The magnetization in the samples in the cyclic range  $\pm 10$  kG do not exhibit hysteresis loop, which indicates that the materials are not ferromagnetic at room temperature. From magnetic moment data, we calculate the values of magnetic susceptibility of S1-S5 which are shown in Table 1. The values of the magnetic susceptibility of the order of  $\sim 10^{-6}$  emu/Gg show weak paramagnetic nature of the materials. Using the Curie law, we calculate the approximate total concentrations of the paramagnetic ions ( $\text{Nd}^{3+} + \text{Co}^{2+}$ ) ions per gram in the samples assuming  $g \sim 2.0$ . Subtracting the values of the concentration of the  $\text{Co}^{2+}$  ions per gram for each sample, obtained by chemical analysis, we obtain the concentration of the  $\text{Nd}^{3+}$  ions per gram in each sample, and the values are shown in Table 1. Absence of ferromagnetism



in the material is due to the low concentrations of the magnetic, viz.  $\text{Co}^{2+}(3d^7)$  and  $\text{Nd}^{3+}(4f^3)$  ions in the amorphous  $\text{SiO}_2$  matrix, in which case the ions are fairly far apart. As a result, ferromagnetic domain formation by long-range spin alignment by d-f interaction through the bridging O 2p orbitals is not feasible.

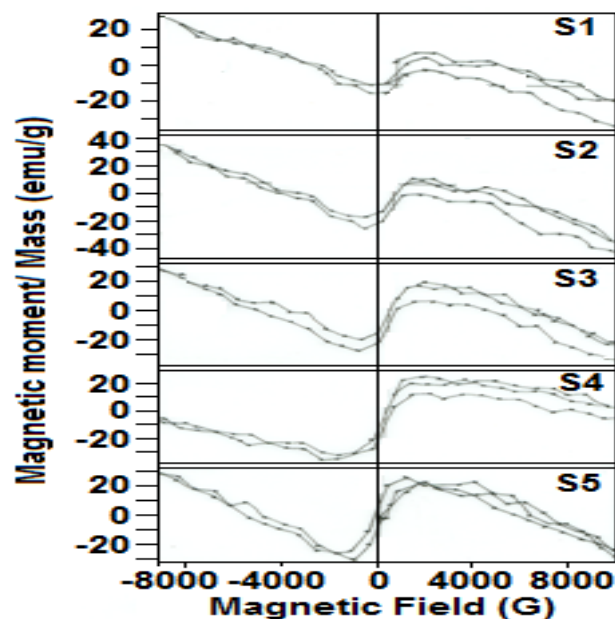


Fig. 4: Plots of the magnetic moment versus magnetic field of the samples S1-S5 of Co- and Nd-doped  $\text{SiO}_2$  system at 300 K

### 3.4 EPR Studies

In Fig. 5(a)-(d), we present the EMR lineshapes of S1-S5 recorded at 6, 50, 77, and 300 K, respectively. The lineshapes are in general very broad and weak, characteristics of complex oxide materials due to very fast spin-lattice relaxation times. The lineshape of sample S1 at 6 K only, exhibits two characteristic peaks with corresponding  $g_{\text{iso}}$ -values  $\sim 2.32$  and  $2.01$  (Table 2). The  $g_{\text{iso}}$ -value  $\sim 2.32$  is due to the  $\text{Co}^{2+}(3d^7)$ ,  $S = 3/2$ ,  $^{59}\text{Co}$ ,  $I = 7/2$ , natural abundance  $\sim 100\%$ ,  $\lambda \sim -172 \text{ cm}^{-1}$ ) ions in tetrahedral coordination with  $^4\text{A}_{2g}(^4\text{F})$  as the ground state [3], [4], and [5]. The peak corresponding to  $g_{\text{iso}}$ -value  $\sim 2.01$  is attributed to the  $\text{Nd}^{3+}(4f^3)$  site [9] in distorted octahedral coordinations. The free ion of  $\text{Nd}^{3+}(4f^3)$  is having  $^4I_{9/2}$  ground state and spin orbit coupling constant,  $\lambda = 300 \text{ cm}^{-1}$  [26]. In a crystal field,  $^4I_{9/2}$  splits up into five, Kramer's doublets, viz.  $9/2$ ,  $7/2$ ,  $5/2$ ,  $3/2$ ,  $1/2$ . Only the lowest doublet is populated at 6 K. Therefore, the system can be described by a pseudo spin  $S = 1/2$ . Nd has three even isotopes with  $I = 0$  and total natural abundances of 79.5%, and two isotopes  $^{143}\text{Nd}$  or  $^{145}\text{Nd}$  ( $I = 7/2$ ) of natural abundances 12.2% and 8.3%, respectively [26]. Therefore, the EPR spectrum of  $\text{Nd}^{3+}$  is expected to be composed of an intense central line due to the even isotopes and a hyperfine pattern with two sets of  $2I + 1 = 8$  lines for the two odd isotopes [9]. However, due to the very low concentrations as well as the low isotopic abundances the of the  $\text{Nd}^{3+}(4f^3)$  ions very poor EMR lineshpes are observed in the complex oxide matrices. The lineshapes further show that the peak corresponding to  $g_{\text{iso}}$ -value  $\sim 2.32$  is smeared out in samples S2-S5 at 6 K, and only the peak corresponding to the  $g_{\text{iso}}$ -value  $\sim 2.01$  persists in S2 through S5 at 6 K. This could be due to the bigger ionic sizes of  $\text{Nd}^{3+}(4f^3)$  ions ( $\text{Nd}^{3+}$  ionic radius  $\sim 0.995 \text{ \AA}$ , 6-coordination;  $\text{Co}^{2+}$  ionic radius  $\sim 0.65 \text{ \AA}$ , 6-coordination) [27] which progressively distorts the  $\text{SiO}_2$  matrix with increasing concentrations. At higher temperatures, at 50, 77, and 300 K, both the peaks in the samples are highly smeared out due to the increasing lattice vibrational frequencies as well as the inverse relationship of the line intensity with temperature [28]. However, we calculate the approximate  $g_{\text{iso}}$ -values of the samples in which ever case it is possible and plausible, within the error limit, and show the values in Table 2.

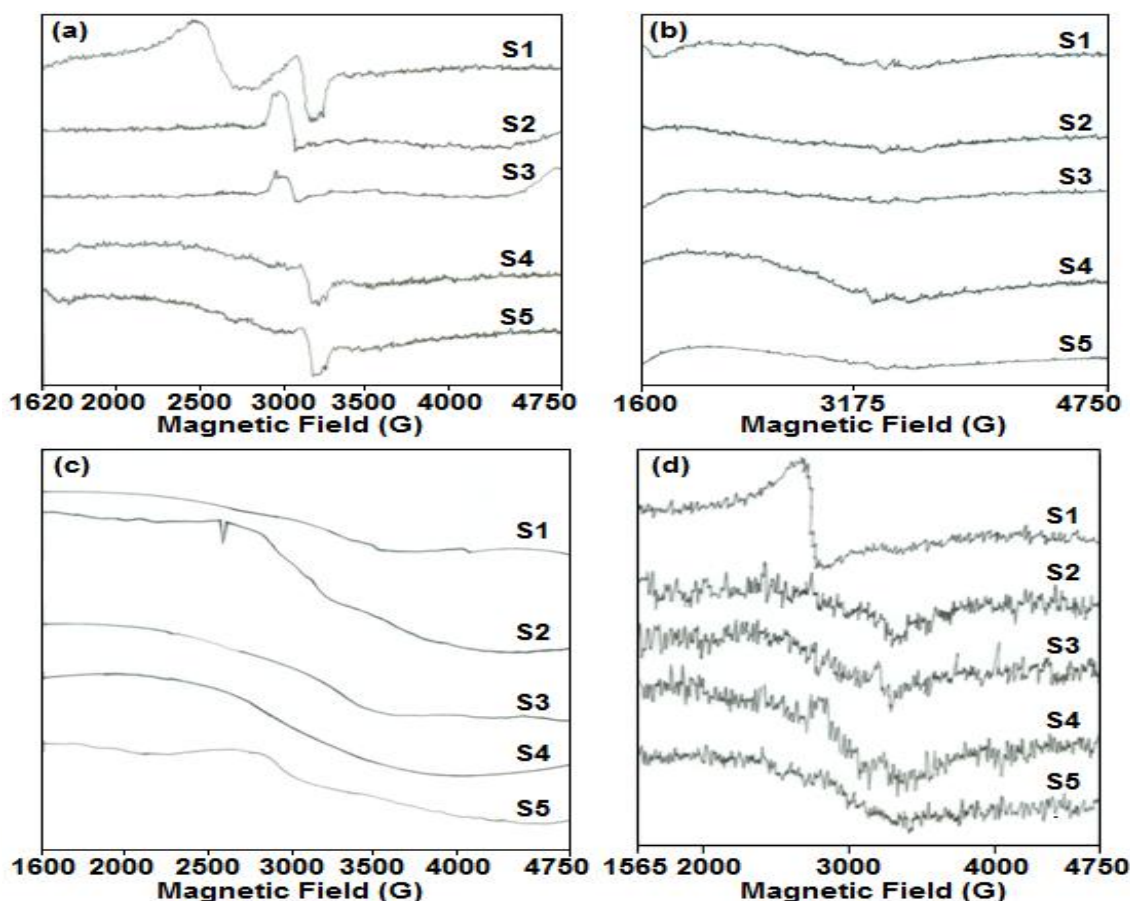


Fig. 5: Observed EMR lineshpes of the samples S1-S5 of Co- and Nd-doped SiO<sub>2</sub> system at (a) 6 K, (b) 50 K, (c) 77 K and (d) 300 K

Table 2. Observed  $g_{iso}$ -values of the samples S1-S5 of Co- and Nd-doped SiO<sub>2</sub> system at 6, 50, 77 and 300 K

Sample No.	6 K		50 K		77 K		300 K	
	$g_{iso}$ -values		$g_{iso}$ -values		$g_{iso}$ -values		$g_{iso}$ -values	
S1	2.32	2.01	-	1.90	-	1.90	2.29	2.04
S2	-	2.01	-	2.08	-	2.08	-	2.01
S3	-	2.01	-	1.97	-	1.97	-	1.90
S4	-	2.01	-	1.97	-	1.97	-	2.01
S5	-	2.01	-	1.80	-	1.80	-	1.61

### 3.5 Optical Absorption Studies

In Fig. 6 we present the room temperature optical absorption spectra of samples S1-S5. The broad signal at  $\sim 750$  nm ( $13262\text{ cm}^{-1}$ ) may be assigned due to transitions of  $^4I_{9/2} \rightarrow ^4F_{7/2} + ^4S_{3/2}$  of optically active Nd<sup>3+</sup> ions in sample [10], [11] and [12]. The trivalent Nd<sup>3+</sup> ion in solids state lose all 5d and 6s electrons. Since optically active 4f electrons are shielded by outer shell d electrons of Nd<sup>3+</sup> ions, the samples are not strongly affected by neighboring ligands [11]. The peak  $\sim 520$  nm ( $19230\text{ cm}^{-1}$ ) is attributed to  $^4A_{2g} \rightarrow ^4T_{1g}(P)$  transitions of Co<sup>2+</sup> ions in weak tetrahedral field [28] which corresponds to a Dq value of  $\sim 400\text{ cm}^{-1}$  as reported by Ballhausen and Jørgensen [3]. The absorptions at lower wavelength are attributed to the charge-transfer bands.



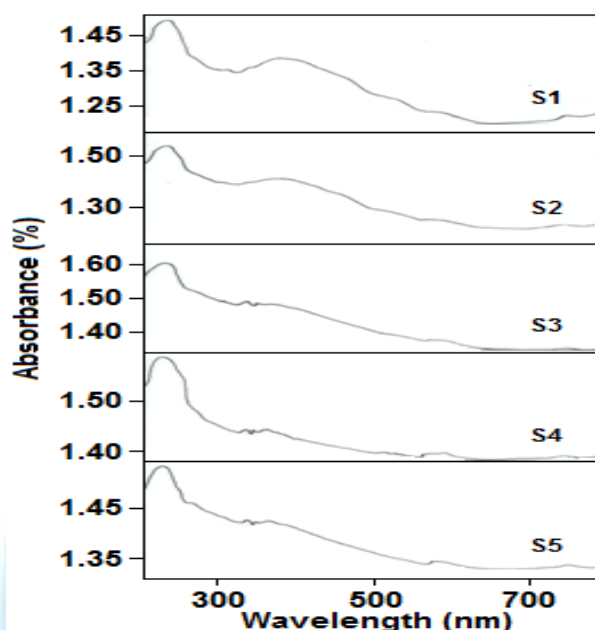


Fig. 6: Optical absorption spectra of the samples S1-S5 of Co- and Nd-doped SiO<sub>2</sub> system at 300 K

#### 4. Conclusion

From our above studies, the following are our major conclusion. Powder XRD results show the formation of amorphous SiO<sub>2</sub> in the samples. DTA-TGA/DTG traces show no phase change and weight loss in the samples in the range 27-700 °C. Room temperature IR results show the presence of octahedral [NdO<sub>6</sub>]<sup>3-</sup>, and tetrahedral [CoO<sub>4</sub>]<sup>4-</sup> and [SiO<sub>4</sub>]<sup>4-</sup> units in the samples. Calculated values of the magnetic susceptibility from the magnetic moments data are found to be  $\sim 10^{-6}$  emu/gG, which show weak paramagnetic nature of the materials. EMR lineshapes recorded at 6, 50, 77 and 300 K show almost smeared out broad and isotropic lineshapes. The only one detectable peak at  $g_{iso}$ -value  $\sim 2.3$  is due to the Co<sup>2+</sup>(3d<sup>7</sup>) ions in tetrahedral coordinations, and the other at  $g_{iso}$ -value  $\sim 2.01$  is due to the Nd<sup>3+</sup>(4f<sup>3</sup>) ions in distorted octahedral coordinations. The above two peaks are distinct only at 6 K, whereas in higher temperatures these peaks are highly smeared out. The optical absorption band at  $\sim 750$  nm (13262 cm<sup>-1</sup>) is assigned to <sup>4</sup>I<sub>9/2</sub> → <sup>4</sup>F<sub>7/2</sub> + <sup>4</sup>S<sub>3/2</sub> transitions in optically active Nd<sup>3+</sup>(4f<sup>3</sup>) ions in octahedral coordinations. The peak  $\sim 520$  nm (19230 cm<sup>-1</sup>) is attributed to <sup>4</sup>A<sub>2g</sub> → <sup>4</sup>T<sub>1g</sub>(P) transitions in Co<sup>2+</sup>(3d<sup>7</sup>) ions in weak tetrahedral field.

#### ACKNOWLEDGMENTS

The authors thank Prof. M. J. Nilges, Illinois EPR Research Centre, University of Illinois, Urbana for help with the EMR data at 50 K at 6 K.

#### REFERENCES

- [1] A. Polman, J. Appl. Phys. 82(1) (July 1997), 1-39.
- [2] Blasse, B., and Grabmier, B.C., 1994. Luminiscent Materials, Springer-Verlag, Heidelberg, pp. 33-70.
- [3] Ballhausen, C.J., 1962. Introduction to Ligand Field Theory, McGraw-Hill Book Company, Inc., London, pp. 256-258.
- [4] Abragam, A., and Bleaney, B., 1970. Electron Paramagnetic Resonance of Transition Ions, Clarendon Press, Oxford, p. 470.
- [5] Figgis, B.N., 1976. Introduction to Ligand Fields, Wiley Eastern Limited, New Delhi, p.307.
- [6] Foglio, M.E., and Barberis, G.E. Study of Co<sup>2+</sup> in different crystal field environments. Braz. J. Phys. 36 (Mar. 2006), 1-32.
- [7] Kojima, K., and Matsuda, J. Electronic spectral study of Co(II) complexes in potassium borate glasses with low alkali oxides, Phys. Chem. Glasses. 29 (August 1988), 154-56.
- [8] Trif, E., and Nicula, A. EPR of Nd<sup>3+</sup> Ions in Y-Type Zeolites. Phys. Stat. Sol. (b) 133 (Feb. 1986), 683-686.
- [9] Guillot-Noel, O., Simons, D., and Gourier, D. EPR study of the multisite character of Nd<sup>3+</sup> ions in zircon-type matrices YMO<sub>4</sub> (M= V, P, As). J. Phys. Chem. Solids 60 (April 1999), 555-565.
- [10] Hu, Z., Lin, Z., Wang, and G. Growth and spectroscopic characterization of Nd<sup>3+</sup>:Sr<sub>6</sub>GdSc(BO<sub>3</sub>)<sub>6</sub> crystal. J. Sol. State Chem., 117 (Sept. 2004), 3028-3031.



- [11] Cernall, W.T., Goodman, G.L., Rajanak, K., and Rana, R.S. A systematic analysis of the spectra of the lanthanides doped into single crystal  $\text{LaF}_3$ . *J. Chem. Phys.* 90 (July 1989), 3443-3453.
- [12] Sardar, D.K., Yow, R.M., Coeckelenbergh, C.H., Sayka, A., and Gruber, J.B. Spectroscopic analysis of  $\text{Nd}^{3+}(4f^3)$  absorption intensities in a plastic host (HEMA). *Polym. Int.* 959 (June 2004), 8103-8108.
- [13] Palanisamy, K. 2014 Sol-Gel Synthesis, Crystal Structure, Electronic and Magnetic Properties of  $\text{A}_{2-x}\text{B}_x\text{C}_{4-3x}\text{O}_7$  ( $0.0 \leq x \leq 0.75$ ) (A= B, Al; B=Pr, As, Gd, Bi; C=Co, Mn) Oxides. Doctoral Thesis. Pondicherry University, India.
- [14] Ramesh, S., and Das, B.B. Synthesis, Structure and Characterization of  $\text{Nd}_{2x}\text{Cd}_{2-3x}\text{SiO}_4$  ( $0.01 \leq x \leq 0.21$ ) Solid-Solutions. *J. Kor. Chem. Soc.* 55 (Mar. 2011), 502-508.
- [15] Das, B.B, Mohanty, D., Yogapriya, M., and Govindarao, R. Sol-Gel Synthesis and Structure-Property Relations in  $\text{Nd}_{4-x}\text{Cs}_{2(1+x)}\text{Fe}_{5-x}\text{Zn}_x\text{O}_{14+\delta}$  ( $0 \leq x \leq 1.0$ ) Oxide Systems. *J. Chem. Chem. Eng.* 5 (Oct. 2011), 962-968
- [16] Hench, L., and West, J.K. The sol-gel process. *Chem Rev.* 90(1) (Jan. 1990), 33-72.
- [17] Ganguli, D. Sol-gel processing: A versatile concept for special glasses and ceramics. *Bull. Mater. Sci.* 16(6) (Dec. 1993), 523-531.
- [18] Brugel, W., 1962. Introduction to IR Spectroscopy, John Wiley and Sons, Inc. New York, p. 228.
- [19] Hocking, M.B., and Mater, S.M. Electron paramagnetic resonance examination of aqueous anthrasemiquinone radical anion. *J. Magn. Res.* 47 (April 1982), 187-199.
- [20] Vogel, A.I., 1967. Text Book of Quantitative Inorganic Analysis Including Elementary Instrumental Analysis, ELBS 5th ed., The English Language Book Society & Longman, Essex, pp. 368-374.
- [21] Q Williams, Mineral Physics and Crystallography, AGU Reference shelf 2, p.291.
- [22] Ladgankar, B. P., Kolekar, C. B., and Vaingankar, A. S. Infrared absorption spectroscopic study of  $\text{Nd}^{3+}$  substituted Zn-Mg ferrites. *Bull. Mater. Sci.* 24 (Aug. 2002), 351-354.
- [23] Nakamoto, K., 1986. Infrared and Raman Spectra of Inorganic and Coordination Compounds, Jahn Wiley and Sons, N.Y., p.139.
- [24] Ref.21, p. 138.
- [25] Atalay, S., Adiguzel, H.I., and Atalay, F. Infrared absorption study of  $\text{Fe}_2\text{O}_3\text{-CaO-SiO}_2$  glass ceramics. *Mat. Sci. Engg.* A304-306 (2001), 796-799.
- [26] Ref. 4, pp. 284-300.
- [27] Shannon, R.D., and Prewitt, C.T. Effective Ionic Radii in Oxides and Fluorides. *Acta. Cryst.* B25 (May 1968), 925-929.
- [28] Bershon, M., and Baird, A.C., 1966. An Introduction to Electron Paramagnetic Resonance. W.A. Benjamin, Inc., New York, p. 47.

## Authors' biography with Photo



Prof. Bidhu Bhusan Das did his 5-Yr. M. Sc. in Chemistry in 1982 and Ph. D. in electron paramagnetic resonance (EPR) and materials chemistry from Indian Institute of Technology Kanpur in 1987. He was a Postdoctoral Fellow (under 35 yrs.) of the Commission of the European Communities in ISMRA Caen during 1992-93 and did his research work in Materials chemistry and powder X-ray crystallography. Prof. Bidhu Bhusan Das served as faculty member in Chemistry in Pondicherry University, Puducherry, University of Hyderabad, Hyderabad and University of Delhi, Delhi in India since 1987. At present, Prof. Bidhu Bhusan Das is a professor in Chemistry in Pondicherry University, Puducherry, India. Prof. Bidhu Bhusan Das has research publications in national and international journals. His research specialization is structure-property relations in electronic and magnetic materials and EPR spectroscopy.



Mr. Ruppa Govinda Rao was born in 9th July, 1983 in Gudem, Srikakulam town, Andhra Pradesh State in India. He attended A.P Residential (B) School, S.M Puram, Andhra Pradesh between 1995-1998, Sri Vikas Junior College, Srikakulam, Andhra Pradesh between 1998-2000 and Sri Rama Degree College, Andhra University, Srikakulam, Andhra Pradesh in India between 2001-2004 where he obtained a Bachelor of Science Degree in Maths, Physics and Chemistry. He obtained his M. Sc. degree in Chemical Sciences from the Department of Chemistry, Pondicherry University, Puducherry, India in 2005-2007. Presently, he is pursuing his Ph.D. research under the guidance of Prof. Bidhu Bhusan Das, in Functional Materials Chemistry, Department of Chemistry, Pondicherry University, Puducherry, India. His research interests are sol-gel synthesis, crystal structure, magnetic, electronic and optical properties of nanoxides.